Published in final edited form as:
J Thromb Haemost. 2008 August ; 6(8): 1344–1351. doi:10.1111/j.1538-7836.2008.03033.x.

TFPIγ is an Active Alternatively Spliced Form of TFPI Present in Mice but not in Humans

Susan A. Maroney[1], **Josephine P. Ferrel**[1], **Maureen L. Collins**[1], and **Alan E. Mast**[1,2]

[1]Blood Research Institute, Blood Center of Wisconsin, Milwaukee, WI

[2]Department of Cell Biology, Neurobiology and Anatomy, Medical College of Wisconsin, Milwaukee, WI

Abstract

Background—Tissue factor pathway inhibitor (TFPI) is a potent inhibitor of tissue factor procoagulant activity produced as two alternatively spliced isoforms, TFPIα and TFPIβ, which differ in domain structure and mechanism for cell surface association. 3' RACE was used to search for new TFPI isoforms. TFPIγ, a new alternatively spliced form of TFPI was identified and characterized.

Methods—The tissue expression, cell surface association and anticoagulant activity of TFPIγ were characterized and compared to TFPIα and TFPIβ through studies of mouse and human tissues and expression of recombinant proteins in CHO cells.

Results—TFPIγ is produced by alternative splicing using the same 5' splice donor site as TFPIβ and a 3' splice acceptor site 187 nucleotides beyond the stop codon of TFPIβ in exon 8. The resulting protein has the first two Kunitz domains connected to an 18 amino acid C-terminal region specific to TFPIγ. TFPIγ mRNA is differentially produced in mouse tissues but is not encoded within the human TFPI gene. When expressed in CHO cells, TFPIγ is secreted into conditioned media and effectively inhibits tissue factor procoagulant activity.

Conclusions—TFPIγ is a third alternatively spliced form of TFPI widely expressed in mouse tissues but not made by human tissues. It contains the first two Kunitz domains and is a secreted, rather than a cell surface associated protein. It is a functional anticoagulant and may partially explain the resistance of mice to coagulopathy in tissue factor mediated models of disease.

Introduction

Tissue factor (TF) is the primary protein that initiates blood coagulation *in vivo*. TF is typically located on vascular smooth muscle cells, adventitial fibroblasts and pericytes that surround the blood vessel, but not on the surface of endothelial cells or other cells in direct contact with flowing blood (1,2,3). In its extravascular location TF provides a perivascular hemostatic sheath. It binds plasma factor VIIa (fVIIa) following vascular injury; initiates blood coagulation, and thereby prevents severe hemorrhage. However, in inflammatory conditions, TF is expressed within the vasculature by monocytes (4), platelets (5,6) and endothelial cells (7). Intravascular TF can produce intravascular coagulation with potential for the formation of a life threatening occlusive thrombus, as well as cell signaling events thought to mediate, in part, the pathology associated with a wide array of diseases including sepsis (8,9) and tumor metastasis (10,11).

Corresponding Author: Alan E. Mast, Blood Research Institute, PO Box 2178, Milwaukee, WI 53201-2178, Tel: 414-937-6310, Fax: 414-9376284, alan.mast@bcw.edu.

The primary inhibitor of intravascular TF activity is tissue factor pathway inhibitor (TFPI), a protein located on the endothelial surface (12), within platelets (13,14) and in plasma (15,16). Full-length TFPI (called TFPIα) is a 43kD protein consisting of an acidic N-terminal region, followed by three tandem Kunitz-type domains and ending in a basic C-terminal region. The second Kunitz domain directly binds and inactivates factor Xa (fXa), and in a fXa dependent manner, the first Kunitz domain binds and inactivates the TF-fVIIa catalytic complex (17). An alternatively spliced isoform of TFPI, called TFPIβ, has been described (18). In TFPIβ alternative splicing occurs immediately before the third Kunitz domain. Although it contains the first two Kunitz domains present in TFPIα, the alternative splice provides TFPIβ with a different C-terminal region than that of TFPIα. TFPIα and TFPIβ mRNA are present in both humans in mice. To date, no other isoforms of TFPI have been described.

It has been demonstrated in animal models that TF and TFPI directly counterbalance each other *in vivo*, and it is thought that TFPI has a key role in limiting the pathologies associated with intravascular expression of TF (19,9). Our laboratory is interested in murine model systems used to study how TFPI hinders disease processes mediated through intravascular TF activity as correlates for understanding human disease (20). To further understand these model systems, we sought to identify additional TFPI isoforms and characterize their expression in humans and mice. Here, we have used 3' rapid amplification of cDNA ends (3' RACE) to examine human placental and mouse lung cDNA for previously unidentified alternatively spliced forms of TFPI. A new isoform of TFPI, called TFPIγ, is identified which is present in mice but is not in humans.

Methods and Materials

Reagents

Zero Blunt® TOPO® PCR Cloning Kit for Sequencing, Trizol®, pDisplay, Phosphatidylinositol-specific phospholipase C (PIPLC) (Invitrogen, Carlsbad, CA). RNeasy Mini Kit (Qiagen, Valencia, CA, USA), PCR primers (Integrated DNA Technologies, Skokie, IL), rabbit anti-mouse TFPI, Spectrozyme Xa (American Diagnostica, Inc., Greenwich, CT), Human fVIIa, fX, fXa (Enzyme Research, South Bend, IN), Ethyl methanesulfonate, 3,4-dichloroisocoumarin (DCI), E-64 (Sigma Chemical, St. Louis, MO).

3' RACE

Human placenta and mouse (Swiss Webster) lung RACE-ready cDNA (Ambion, Austin, TX) were used to perform 3' RACE PCR reactions. Gene specific primers (Table 1) were produced within regions of human TFPI exons 6 (second Kunitz domain) and 9 (third Kunitz domain) and mouse TFPI exons 6 (second Kunitz domain) and 7 (connecting region between the second and third Kunitz domains). Touchdown PCR was performed twice; first, using the outside gene specific and RACE primers followed by inside gene specific and RACE primers. PCR products were separated using 1% agarose gel electrophoresis and sequenced (Applied Biosystems 3100 Genetic Analyzer). Additional sequencing was performed following PCR product insertion into Zero Blunt® TOPO® and transformation into DH5α *E. coli*.

Real time PCR for TFPIα and TFPIβ in human and mouse tissues

Human total tissue RNA was purchased from Clontech (Mountain View, CA). To obtain mouse tissue RNA, BALB/c or C57BL/6 mice were perfused with sterile PBS, tissues harvested, and immediately placed in RNA later® at −80°C. Total RNA was isolated in Trizol® reagent and further purified using RNeasy Mini Kit. Human and mouse cDNA was produced from 2 μg of total RNA in Superscript II with oligo-dT primers. Gene specific

primers for human and mouse TFPIα and TFPIβ were selected using Primer Quest (Intergrated DNA Technologies, Coralville, IA) (Table 1). Assays were normalized to ribosomal protein L-19 on 7500 Real-Time PCR System (Applied Biosystem, Foster City, CA) using SYBER® Green.

Detection of TFPIγ mRNA in human and mouse tissues

Human and mouse cDNA was produced as described above. Primers to human and mouse TFPI were selected to identify alternative splice sites in exon 8 of the human and mouse TFPI genes (Table 1).

Flow cytometry of CHO cells transfected with TFPI isoforms

To characterize TFPIγ, mouse TFPIα, TFPIβ, and TFPIγ constructs were produced, inserted into pDisplay, and transfected into Chinese hamster ovary (CHO) cells. Stable transfected CHO cells each containing one of the three TFPI isoforms were analyzed by flow cytometry following PIPLC treatment at 1 U/ml for 30 min at 37°C or heparin treatment at 1 U/ml for 30 min at 23°C. Cells were harvested with 5mM EDTA, fixed with 1.5% formaldehyde, incubated with 10μg/ml rabbit anti-mouse TFPI followed by anti-rabbit IgG FITC, and re-suspended in PBS with 0.1% BSA (PBSA) for analysis. Flow cytometry was performed using FACScan II (Becton Dickinson, Mountain View, CA) running WinMDI 2.8 software.

TFPI activity assays

Functional TFPI activity was determined by measurement of fX activation by TF-fVIIa as previously described (21). Briefly, a 200 μl aliquot of standardized, harvested cells was treated with 1U/ml PIPLC for 1 hr at 37°C. TFPI activity in the PIPLC supernatant and corresponding conditioned media was determined by assay with 0.2 nM human fVIIa, 20 nM human fX and a 1:10,000 dilution of recombinant human tissue factor (RecombinPlasTin, Instrumentation Laboratory, Lexington, MA). After 30 minutes the reaction was quenched with 20 mM EDTA. FXa generated was determined using 500 μM fXa substrate. TFPI in the samples was quantified by comparison to a standard curve generated using known amounts of recombinant TFPI.

TFPI precipitation and SDS-PAGE and western blot analysis

TFPI isoform transfected CHO cells and mouse tissues were lysed in 30μM CHAPS detergent containing DCI (10μM), EDTA (10μM), and E-64 (1μM). Following centrifugation (20,000g, 10 min) to remove cellular debris, TFPI was precipitated from protein standardized cellular lysates using bovine fXa agarose (1 hour, 4°C). The agarose beads were washed, boiled in SDS sample buffer, and the supernatant subjected to 10% SDS-PAGE and western blot analysis for TFPI.

Results

3’ RACE of human placental cDNA identifies TFPIα and TFPIβ

The 3’RACE PCR reaction using human placental cDNA and 5’ primers designed to anneal with regions of the second Kunitz domain (Table 1) produced four major products (Figure 1A). Nucleotide sequence analysis identified the top two bands as TFPIα and the bottom two bands as TFPIβ. When the 3’RACE reaction was repeated using 5’ primers targeting the third Kunitz domain (Table 1), only TFPIα was identified (data not shown). Since sequencing of the major 3’RACE PCR products did not identify any new human TFPI isoforms, the 3’RACE PCR products were cloned into E. coli. Purified plasmids from individual transformed colonies were subjected to nucleotide sequence analysis. Of 107

colonies analyzed, 73% contained TFPIα and 27% contained TFPIβ. Again, no new human TFPI isoforms were identified.

3' RACE of mouse lung cDNA identifies TFPIα, TFPIβ and a third TFPI isoform

3' RACE of mouse lung cDNA using 5' primer sets designed to anneal with regions of the second Kunitz domain (Table 1) produced five major PCR products (Figure 1A). Nucleotide sequence analysis identified the top two bands as TFPIα and the next two bands as TFPIβ. Despite repeated attempts, direct nucleotide analysis of the fifth band was not successful. We considered the possibility that the fifth band represents a previously undiscovered alternatively spliced form of TFPI. A search of the genebank database revealed sequence of a third isoform of TFPI present in mice but not humans (Genebank AK034752). We have named this isoform TFPIγ. The alternative splicing in TFPIγ occurs at the same 5' splice donor site as TFPIβ. Therefore, TFPIγ has the first two Kunitz domains, the functional regions on TFPI necessary for binding and inactivation of fVIIa and fXa. The 3' splice acceptor of TFPIγ is located 187 nucleotides downstream of the TFPIβ stop codon within Exon 8 of TFPI. The unique C-terminal region encodes 18 amino acids (Figure 1B).

The unique C-terminal sequence of mouse TFPIγ was used to BLAST for similar sequence in other species in the NCBI data base. No homologous sequence was identified in human, chimpanzee, rhesus monkey, rat, dog, cow or horse. Thus, it appears that TFPIγ is specific to mice and likely arose through exonization of mouse sequence rather than exon loss from other species.

TFPIγ is expressed in mouse tissues but not human tissues

Human exon 8 is much smaller than mouse exon 8 and does not contain a homologous TFPIγ coding region (Figure 1B). Human placental and kidney cDNA was examined to confirm the absence of TFPIγ in humans. PCR reactions using a forward primer annealing with a region of the second Kunitz domain and reverse primers annealing with either a distal region of exon 8 (to amplify TFPIβ and TFPIγ) or the C-terminal region of TFPIα (to amplify TFPIα) were performed using human and mouse cDNA (Table 1). When human placenta or kidney cDNA was used, one major PCR product was present in each of the two reactions. Nucleotide sequence analysis identified these as TFPIβ (Figure 2, Lane 1) and TFPIα (Figure 2, Lane 2). When mouse cDNA from either BALB/c or C57BL/6 mice was used as the template, two major PCR products were present in the reaction using the 3' primer annealing with a region of exon 8 (Figure 2, Lane 3). Nucleotide sequence analysis identified the bands as TFPIβ (top band) and TFPIγ (bottom band). One major product was present in the reaction using the 3' primer annealing with the third Kunitz domain consistent with amplification of TFPIα (Figure 2, Lane 4).

TFPIα mRNA is more abundant than TFPIβ mRNA in mouse tissues

Since sequence encoding TFPIγ is in the 3' untranslated region of TFPIβ mRNA, TFPIγ mRNA cannot be quantified using real time PCR without also measuring TFPIβ mRNA. Quantitative PCR analysis can be used to specifically measure TFPIα and TFPIβ mRNA in human and mouse tissues (Figure 3A). The amount of TFPIβ mRNA in different tissues is consistently less than that of TFPIα mRNA by 3.8- to 22.4-fold in humans and 4.4- to 51.3-fold in mice (Figure 3B).

TFPIβ and TFPIγ mRNA are differentially expressed in mouse tissues

Since both TFPIβ and TFPIγ PCR products can be produced in a single reaction, the intensity of the bands is a reasonable indicator of the amount of TFPIβ and TFPIγ mRNA made by different mouse tissues. Both isoforms are expressed in all nine tissues examined

(Figure 3C). More TFPIγ mRNA is produced by all tissues except heart and testicle that produce more TFPIβ mRNA. TFPIγ mRNA is at most 2-fold more abundant than TFPIβ mRNA; comparison with the TFPIα and TFPIβ real time PCR results indicates that TFPIα mRNA is more prevalent than TFPIγ mRNA in all tissues.

TFPIγ is secreted when expressed in CHO cells and inhibits TF-fVIIa activity

The alternatively spliced C-terminal amino acids of TFPIβ encode a glycosyl phosphatidylinositol (GPI) anchor attachment sequence that directly attaches it to the cell surface (22). To determine if the alternatively spliced C-terminal amino acids of TFPIγ encode a GPI-anchor attachment sequence, stable CHO cell lines expressing each of the three mouse TFPI isoforms were produced and examined for surface TFPI using flow cytometry (Figure 4A). Cells transfected with TFPIβ have mean fluorescence intensity (MFI) 3- to 5-fold higher than cells expressing either TFPIα or TFPIγ. Following treatment with PIPLC, an enzyme that specifically removes GPI-anchored proteins from the cell surface, surface expression of TFPIβ is dramatically reduced, consistent with its GPI-anchor. The amount of TFPIα and TFPIγ on the cell surface also decreases by about one-half following treatment with PIPLC. A similar small amount of surface binding and decrease with PIPLC treatment has been observed in CHO cells transfected with human TFPIα (22). Incubation of the cells with 1 U/ml heparin had no effect on the amount of surface TFPIα, TFPIβ or TFPIγ (data not shown). TFPIγ produced by CHO cells inhibits TF-fVIIa mediated generation of fXa and this inhibitory activity can be reversed using an anti-mouse TFPI antibody (Figure 4B). TFPI activity assays were used to determine the relative amounts of each TFPI isoform secreted into conditioned media versus that removed from the cell surface with PIPLC. The proportion of TFPI removed from the cell surface by PIPLC is 4- to 5-fold higher for cells transfected with TFPIβ than for cells transfected with either TFPIα or TFPIγ (Figure 4C). The combined data from the flow cytometry and TFPI activity assays indicate that TFPIα and TFPIγ are primarily processed as secreted proteins by CHO cells while TFPIβ is primarily processed as a GPI-anchored protein.

Production of TFPIγ protein in mouse tissues

Differentiation of TFPIα and TFPIβ protein is difficult because: 1) these two isoforms migrate at the same molecular weight in SDS-PAGE and 2) the lack of high affinity antibodies that specifically recognize the individual isoforms (22). An antibody directed against the unique C-terminal amino acids of TFPIγ was produced. However, as with antibodies made against the unique C-terminal amino acids of TFPIβ, this antibody does not recognize TFPIγ from transfected CHO cells. As an alternative, the mouse TFPI isoforms from the transfected CHO cells were examined with a polyclonal anti-mouse TFPI antibody. These studies demonstrated that mouse TFPIα and TFPIβ migrate at the same molecular weight (as has been observed for the human proteins (22)). In contrast, TFPIγ migrates as three bands, one of which is distinctly smaller than either TFPIα or TFPIβ (Figure 5). It is unclear why TFPIγ migrates as three bands, but may represent different amounts of glycosylation. Western blots of TFPI in different mouse tissues were compared to the recombinant isoforms made in the CHO cells (Figure 5). Several of the tissues contain a lower molecular weight band that corresponds in size with the lower molecular weight band of TFPIγ in the transfected CHO cells suggesting that small amounts of TFPIγ protein is present within mouse tissues. However, this lower molecular weight band may represent a degradation product. Further studies are needed to definitively identify the production of TFPIγ protein in mouse tissues.

Discussion

TFPIα and TFPIβ are the two TFPI isoforms previously identified and characterized. Both isoforms are present in human and mouse. They have distinct differences in their protein structure and mechanism for cell surface association (22). TFPIα has a third Kunitz domain and highly basic C-terminal region, which are not present in TFPIβ, and indirectly associates with the endothelial surface through binding a GPI-anchored co-receptor (23,24,22,21). The third Kunitz domain does not appear to function as a protease inhibitor, but it may have an important role in the association of TFPIα with the endothelial surface (25). The C-terminal region of TFPIβ encodes a GPI-anchor attachment sequence that directly attaches it to the endothelial surface (22). Solution phase studies have demonstrated that the third Kunitz domain and C-terminal region of TFPIα enhance fXa inhibition when compared to altered forms of TFPI containing only the first two Kunitz domains suggesting that TFPIα is a much more potent anticoagulant than TFPIβ *in vivo* (26,27). However, studies of an altered form of TFPI containing only the first two Kunitz domains, and therefore similar to TFPIβ, demonstrated that its anticoagulant activity increased 250-fold when it was linked to annexin V to create a chimeric protein with high affinity for phosphatidylserine containing membranes (28). Thus, it remains unclear how these structural differences between TFPIα and TFPIβ correlate with their physiological functions. This uncertainty led us to perform 3'RACE experiments to determine if additional alternatively spliced forms of TFPI are made. We initially were interested in determining if an alternatively spliced form of TFPI containing the third Kunitz domain and a direct GPI-anchor attachment sequence could be identified. While no evidence for this form of TFPI was found, a new alternatively spliced isoform of TFPI, called TFPIγ, that is produced in mouse, but not human, tissues was identified.

TFPIγ is spliced immediately preceding K3 at the same 5' splice donor site as TFPIβ. The 3' splice acceptor site (CTCTTAACAG) for TFPIγ is 280 nucleotides downstream from the end of TFPIβ in exon 8 such that the coding region for TFPIγ is in the 3' untranslated region of TFPIβ. There is a predicted splicing branch site sequence (CTGAT) 64 nucleotides upstream from the start of the TFPIγ coding region. The entire 3' untranslated region of human TFPIβ is only 98 nucleotides, compared with 1301 nucleotides in mouse, explaining why TFPIγ is not present in humans. The alternative splicing provides TFPIγ with an 18 amino acid, C-terminal region different from that present in either TFPIα or TFPIβ.

All three alternatively spliced mouse isoforms are expressed in all tissues examined. TFPIα mRNA is more abundant than both TFPIβ and TFPIγ mRNA in all tissues. TFPIγ mRNA is more prevalent than TFPIβ mRNA in all tissues except heart and testicle. This tissue specific pattern of expression of GPI-anchored (TFPIβ) and soluble (TFPIγ) forms of TFPI within vascular beds is interesting because the heart and testicle are two tissues prone to hemorrhage in mice expressing low amounts of TF (29,30).

When TFPIγ is expressed in CHO cells, only about 2% localizes on the cell surface while 98% is secreted into the conditioned media. This behavior is essentially identical to TFPIα and distinctly different from TFPIβ, demonstrating that the C-terminal region of TFPIγ does not encode a GPI-anchor attachment sequence. CHO cells express very low amounts of the GPI-anchored co-receptor that localizes TFPIα to the endothelial surface (22). Since TFPIγ lacks the third Kunitz domain and basic C-terminal region that are thought to be important for localization of TFPIα to the endothelial surface, (25) it is likely that TFPIγ is secreted by endothelial cells *in vivo*. However, the flow cytometry data presented in Figure 4A demonstrate that small amounts of TFPIγ are on the CHO cell surface and are removed by PIPLC, again in a manner almost identical to that observed for TFPIα. These data suggest

that a mechanism for indirect attachment of TFPI to the CHO cell surface that does not require the third Kunitz domain or basic C-terminal region may exist.

TFPIγ made by CHO cells inhibits the activation of fX by fVIIa-TF, demonstrating that it is a functional anticoagulant. Polyclonal antisera directed against the unique amino acids in TFPIγ did not react with TFPIγ made in CHO cells, and we were unable to directly demonstrate production of TFPIγ by western blot. Previous studies have demonstrated that human TFPIα and TFPIβ migrate as the same molecular weight on SDS-PAGE but differently following deglycosylation. Deglycosylation of mouse TFPIα, TFPIβ, and TFPIγ causes TFPIα and TFPIβ to migrate at different molecular weight in a similar manner to the human protein. However, deglycosylated mouse TFPIβ and TFPIγ migrate at nearly identical molecular weight (JPF and AEM unpublished data) limiting the usefulness of this technique to specifically identify TFPIγ in mouse tissues or plasma. Examination of non-deglycosylated mouse tissues by western blot demonstrates a unique low molecular weight band corresponding to a band present in non-deglycosylated TFPIγ but not in TFPIα or TFPIβ. Therefore, this band only suggests that TFPIγ may be made in mouse tissues and further studies will be needed to definitively quantify the relative production of TFPIα, TFPIβ and TFPIγ protein in different tissues. In addition, the low molecular weight band was only observed when the gels were relatively overloaded. It appears that TFPIα and/or TFPIβ, are the predominant isoforms present in mouse tissues.

Alternative splicing of pre-RNA allows the production of structurally and functionally distinct protein isoforms from a single gene. Species specific splicing, such as occurs with TFPIγ, typically is considered a relatively recent evolutionary event in which small amounts of the alternatively spliced isoform are produced with little physiological impact (31). However, these isoforms also may alter species specific physiology by producing low levels of a protein with unique function and/or by regulating the expression of other splice isoforms through sequestration of nucleic acid binding proteins (31). The anticoagulant activity of TFPIγ may explain some of the species specific discrepancies identified when comparing mouse models of TF function to human disease. For example, mice are resistant to myocardial infarction in models of atherosclerotic plaque rupture and even highly prothrombotic mice with factor V Leiden or antithrombin deficiency do not develop deep venous thrombosis in their extremities (32,33,34). Activation of coagulation with associated tissue fibrin deposition following injection of lipopolysaccharide also is much less pronounced in mice than in non-human primates. In a baboon model of E. coli induced sepsis decreased TFPI activity directly contributes to sepsis induced coagulation and tissue fibrin deposition (9) suggesting that production of TFPIγ by mice may partially explain their resistance to sepsis induced coagulopathy. In addition, many therapeutic agents have successfully dampened the adverse effects of sepsis in animal models but have failed in human trials. Explanations for the discrepancy between the mouse studies and human trials are varied and include the use of young mice without underlying disease and the use of well defined organisms rather than mixed infections (35). However, understanding the differences in the function of proteins of the hemostatic systems of humans and mice may provide a more satisfying explanation for these discrepancies. The identification and initial characterization of TFPIγ as an additional isoform of TFPI expressed in mice but not humans moves us one step forward in this process.

References

1. Drake TA, Morrissey JH, Edgington TS. Selective cellular expression of tissue factor in human tissues. Implications for disorders of hemostasis and thrombosis. Am J Pathol. 1989; 134:1087–1097. [PubMed: 2719077]

2. Fleck RA, Rao LV, Rapaport SI, Varki N. Localization of human tissue factor antigen by immunostaining with monospecific, polyclonal anti-human tissue factor antibody. Thromb Res. 1990; 59:421–437. [PubMed: 2237820]

3. Flossel C, Luther T, Muller M, Albrecht S, Kasper M. Immunohistochemical detection of tissue factor (TF) on paraffin sections of routinely fixed human tissue. Histochemistry. 1994; 101:449–453. [PubMed: 7960944]

4. Drake TA, Ruf W, Morrissey JH, Edgington TS. Functional tissue factor is entirely cell surface expressed on lipopolysaccharide-stimulated human blood monocytes and a constitutively tissue factor-producing neoplastic cell line. J Cell Biol. 1989; 109:389–395. [PubMed: 2663880]

5. Schwertz H, Tolley ND, Foulks JM, Denis MM, Risenmay BW, Buerke M, Tilley RE, Rondina MT, Harris EM, Kraiss LW, Mackman N, Zimmerman GA, Weyrich AS. Signal-dependent splicing of tissue factor pre-mRNA modulates the thrombogenecity of human platelets. J Exp Med. 2006; 203:2433–2440. [PubMed: 17060476]

6. Panes O, Matus V, Saez CG, Quiroga T, Pereira J, Mezzano D. Human platelets synthesize and express functional tissue factor. Blood. 2007; 109:5242–5250. [PubMed: 17347408]

7. Mackman N, Tilley RE, Key NS. Role of the extrinsic pathway of blood coagulation in hemostasis and thrombosis. Arterioscler Thromb Vasc Biol. 2007; 27:1687–1693. [PubMed: 17556654]

8. Pawlinski R, Mackman N. Tissue factor, coagulation proteases, and protease-activated receptors in endotoxemia and sepsis. Crit Care Med. 2004; 32:S293–S297. [PubMed: 15118533]

9. Tang H, Ivanciu L, Popescu N, Peer G, Hack E, Lupu C, Taylor FB Jr, Lupu F. Sepsis-Induced Coagulation in the Baboon Lung Is Associated with Decreased Tissue Factor Pathway Inhibitor. Am J Pathol. 2007; 171:1066–1077. [PubMed: 17640967]

10. Ruf W, Mueller BM. Thrombin generation and the pathogenesis of cancer. Semin Thromb Hemost. 2006; 32(Suppl 1):61–68. [PubMed: 16673267]

11. Versteeg HH, Schaffner F, Kerver M, Petersen HH, Ahamed J, Felding-Habermann B, Takada Y, Mueller BM, Ruf W. Inhibition of tissue factor signaling suppresses tumor growth. Blood. 2008; 111:190–199. [PubMed: 17901245]

12. Bajaj MS, Kuppuswamy MN, Saito H, Spitzer SG, Bajaj SP. Cultured Normal Human Hepatocytes do not Synthesize Lipoprotein-Associated Coagulation Inhibitor: Evidence that Endothelium is the Principal Site of Its Synthesis. PNAS. 1990; 87:8869–8873. [PubMed: 2247459]

13. Novotny WF, Girard TJ, Miletich JP, Broze GJ Jr. Platelets secrete a coagulation inhibitor functionally and antigenically similar to the lipoprotein associated coagulation inhibitor. Blood. 1988; 72:2020–2025. [PubMed: 3143429]

14. Maroney SA, Haberichter SL, Friese P, Collins ML, Ferrel JP, Dale GL, Mast AE. Active tissue factor pathway inhibitor is expressed on the surface of coated platelets. Blood. 2007; 109:1931–1937. [PubMed: 17082321]

15. Novotny WF, Girard TJ, Miletich JP, Broze GJ Jr. Purification and characterization of the lipoprotein-associated coagulation inhibitor from human plasma. J Biol Chem. 1989; 264:18832–18837. [PubMed: 2553722]

16. Sandset PM, Abildgaard U, Larsen ML. Heparin induces release of extrinsic coagulation pathway inhibitor (EPI). Thromb Res. 1988; 50:803–813. [PubMed: 3413731]

17. Girard TJ, Warren LA, Novotny WF, Likert KM, Brown SG, Miletich JP, Broze GJ Jr. Functional significance of the Kunitz-type inhibitory domains of lipoprotein-associated coagulation inhibitor. Nature. 1989; 338:518–520. [PubMed: 2927510]

18. Chang JY, Monroe DM, Oliver JA, Roberts HR. TFPIbeta, a second product from the mouse tissue factor pathway inhibitor (TFPI) gene. Thromb Haemost. 1999; 81:45–49. [PubMed: 9974373]

19. Pedersen B, Holscher T, Sato Y, Pawlinski R, Mackman N. A balance between tissue factor and tissue factor pathway inhibitor is required for embryonic development and hemostasis in adult mice. Blood. 2005; 105:2777–2782. [PubMed: 15598816]

20. Maroney SA, Cooley BC, Sood R, Weiler H, Mast AE. Combined tissue factor pathway inhibitor and thrombomodulin deficiency produces an augmented hypercoagulable state with tissue-specific fibrin deposition. Journal of Thrombosis and Haemostasis. 2008; 6:111–117. [PubMed: 17973652]

21. Maroney SA, Cunningham AC, Ferrel J, Hu R, Haberichter S, Mansbach CM, Brodsky RA, Dietzen DJ, Mast AE. A GPI-anchored co-receptor for tissue factor pathway inhibitor controls its

intracellular trafficking and cell surface expression. Journal of Thrombosis and Haemostasis. 2006; 4:1114–1124. [PubMed: 16689766]

22. Zhang J, Piro O, Lu L, Broze GJ Jr. Glycosyl phosphatidylinositol anchorage of tissue factor pathway inhibitor. Circulation. 2003; 108:623–627. [PubMed: 12835228]
23. Sevinsky JR, Rao LV, Ruf W. Ligand-induced protease receptor translocation into caveolae: a mechanism for regulating cell surface proteolysis of the tissue factor- dependent coagulation pathway. J Cell Biol. 1996; 133:293–304. [PubMed: 8609163]
24. Lupu C, Goodwin CA, Westmuckett AD, Emeis JJ, Scully MF, Kakkar VV, Lupu F. Tissue factor pathway inhibitor in endothelial cells colocalizes with glycolipid microdomains/caveolae. Regulatory mechanism(s) of the anticoagulant properties of the endothelium. Arterioscler Thromb Vasc Biol. 1997; 17:2964–2974. [PubMed: 9409283]
25. Piro O, Broze GJ Jr. Role for the Kunitz-3 Domain of Tissue Factor Pathway Inhibitor-{alpha} in Cell Surface Binding. Circulation. 2004; 110:3567–3572. [PubMed: 15557366]
26. Lockett JM, Mast AE. Contribution of regions distal to glycine-160 to the anticoagulant activity of tissue factor pathway inhibitor. Biochemistry. 2002; 41:4989–4997. [PubMed: 11939795]
27. Petersen JG, Meyn G, Rasmussen JS, Petersen J, Bjorn SE, Jonassen I, Christiansen L, Nordfang O. Characterization of human tissue factor pathway inhibitor variants expressed in Saccharomyces cerevisiae. J Biol Chem. 1993; 268:13344–13351. [PubMed: 8514773]
28. Chen HH, Vicente CP, He L, Tollefsen DM, Wun TC. Fusion proteins comprising annexin V and Kunitz protease inhibitors are highly potent thrombogenic site-directed anticoagulants. Blood. 2005:2004–2011. [PubMed: 16269616]
29. Snyder LA, Rudnick KA, Tawadros R, Volk A, Tam SH, Anderson GM, Bugelski PJ, Yang J. Expression of human tissue factor under the control of the mouse tissue factor promoter mediates normal hemostasis in knock-in mice. Journal of Thrombosis and Haemostasis. 2008; 6:306–314. [PubMed: 18005233]
30. Mackman N. Tissue-specific hemostasis: role of tissue factor. Journal of Thrombosis and Haemostasis. 2008; 6:303–305. [PubMed: 18088348]
31. Xing Y, Lee C. Alternative splicing and RNA selection pressure--evolutionary consequences for eukaryotic genomes. Nat Rev Genet. 2006; 7:499–509. [PubMed: 16770337]
32. Rak J, Yu JL, Luyendyk J, Mackman N. Oncogenes, trousseau syndrome, and cancer-related changes in the coagulome of mice and humans. Cancer Res. 2006; 66:10643–10646. [PubMed: 17108099]
33. Dewerchin M, Herault JP, Wallays G, Petitou M, Schaeffer P, Millet L, Weitz JI, Moons L, Collen D, Carmeliet P, Herbert JM. Life-threatening thrombosis in mice with targeted Arg48-to-Cys mutation of the heparin-binding domain of antithrombin. Circ Res. 2003; 93:1120–1126. [PubMed: 14592998]
34. Lusis AJ. Atherosclerosis. Nature. 2000; 407:233–241. [PubMed: 11001066]
35. Esmon CT. Why do animal models (sometimes) fail to mimic human sepsis? Crit Care Med. 2004; 32:S219–S222. [PubMed: 15118521]

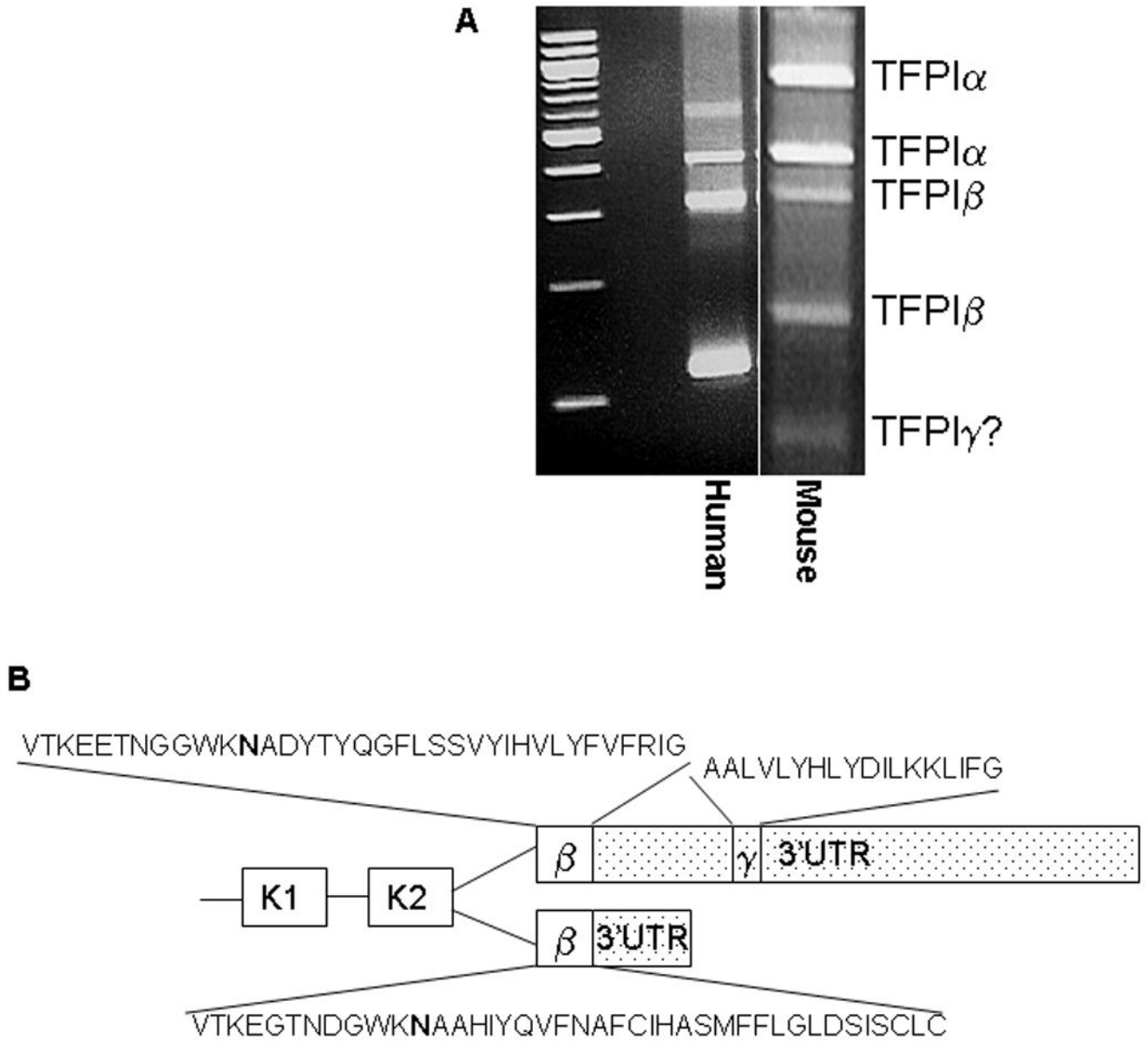

Figure 1.

TFPIγ is a third alternatively spliced form of TFPI. A) DNA gel electrophoresis of 3' RACE products from human placenta and mouse lung. A fifth band that may represent TFPIγ is present in the mouse reaction that was not observed in the human reaction. B) Schematic diagram comparing alternative splicing within exon 8 of human and mouse TFPI. Both human and mouse produce TFPIβ by reading through exon 7 directly into exon 8. TFPIγ is within the 3' untranslated region (3'UTR) of TFPIβ (stippled) and is produced only in mouse tissues by reading through exon 7 with alternative splicing distal to the TFPIβ stop codon in exon 8. The amino acid sequences of the unique C-terminal regions of human and mouse TFPIβ and mouse TFPIγ are indicated. The asparagine (N) residue that serves as the predicted GPI-anchor attachment site in TFPIβ is in bold type.

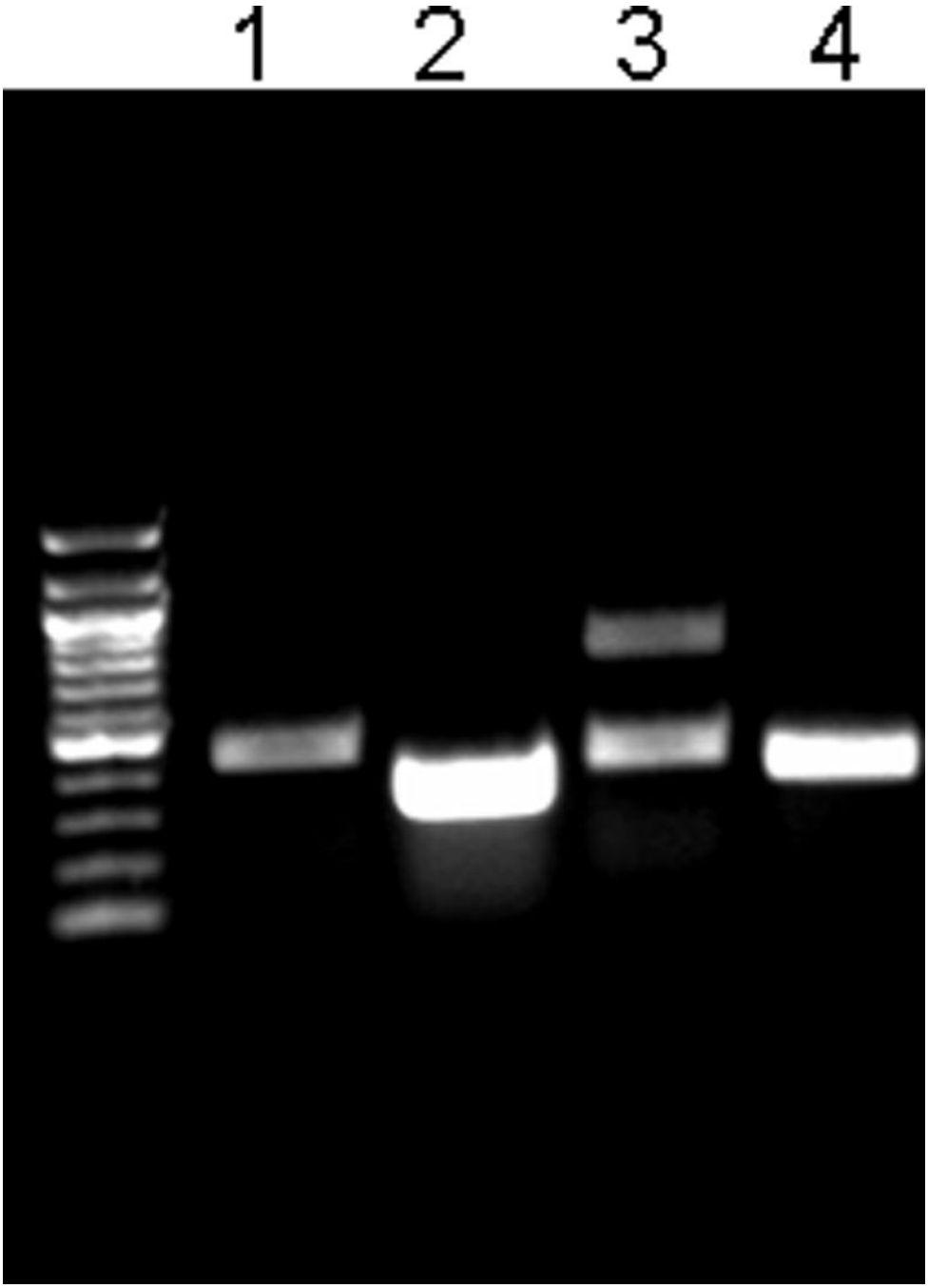

Figure 2.
TFPIγ mRNA is produced in mouse but not human tissues. DNA gel electrophoresis of PCR products from reactions designed to amplify TFPIα (5' primer in second Kunitz domain; 3' primer in C-terminal region of TFPIα) or TFPIβ and TFPIγ (5' primer in the second Kunitz domain; 3' primer in distal end of exon 8). Lane 1 – human TFPIβ (TFPIγ is not observed); Lane 2 – human TFPIα; Lane 3 – mouse TFPIβ and TFPIγ; Lane 4 – mouse TFPIα. Identical results were obtained using cDNA from human kidney and placenta.

A

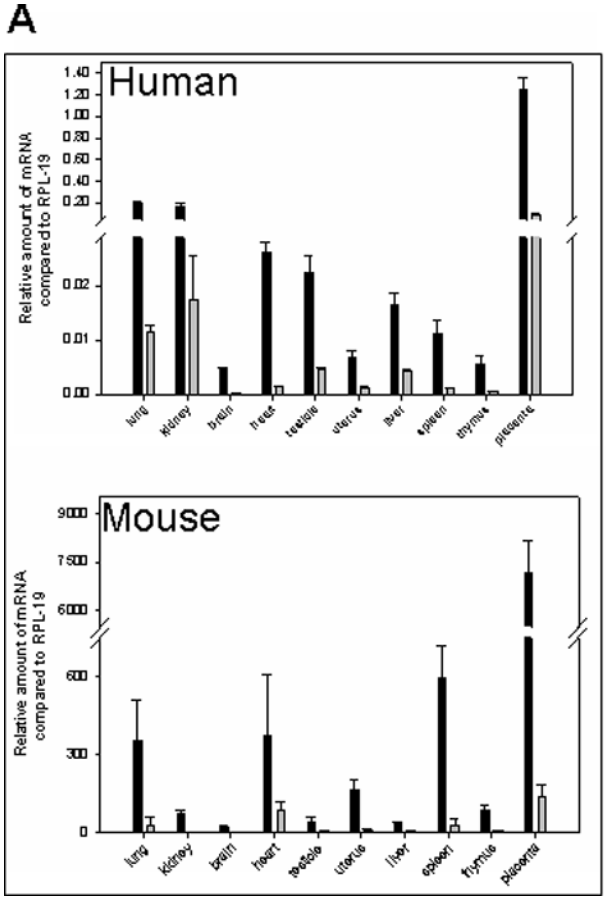

B

Tissue	Human TFPIα/TFPIβ	Mouse TFPIα/TFPIβ
Lung	17.54	11.32
Kidney	9.54	21.18
Brain	22.38	9.33
Heart	17.88	4.40
Testicle	4.91	7.44
Uterus	5.38	17.39
Liver	3.77	5.75
Spleen	10.77	21.05
Thymus	12.94	9.29
Placenta	14.40	51.29

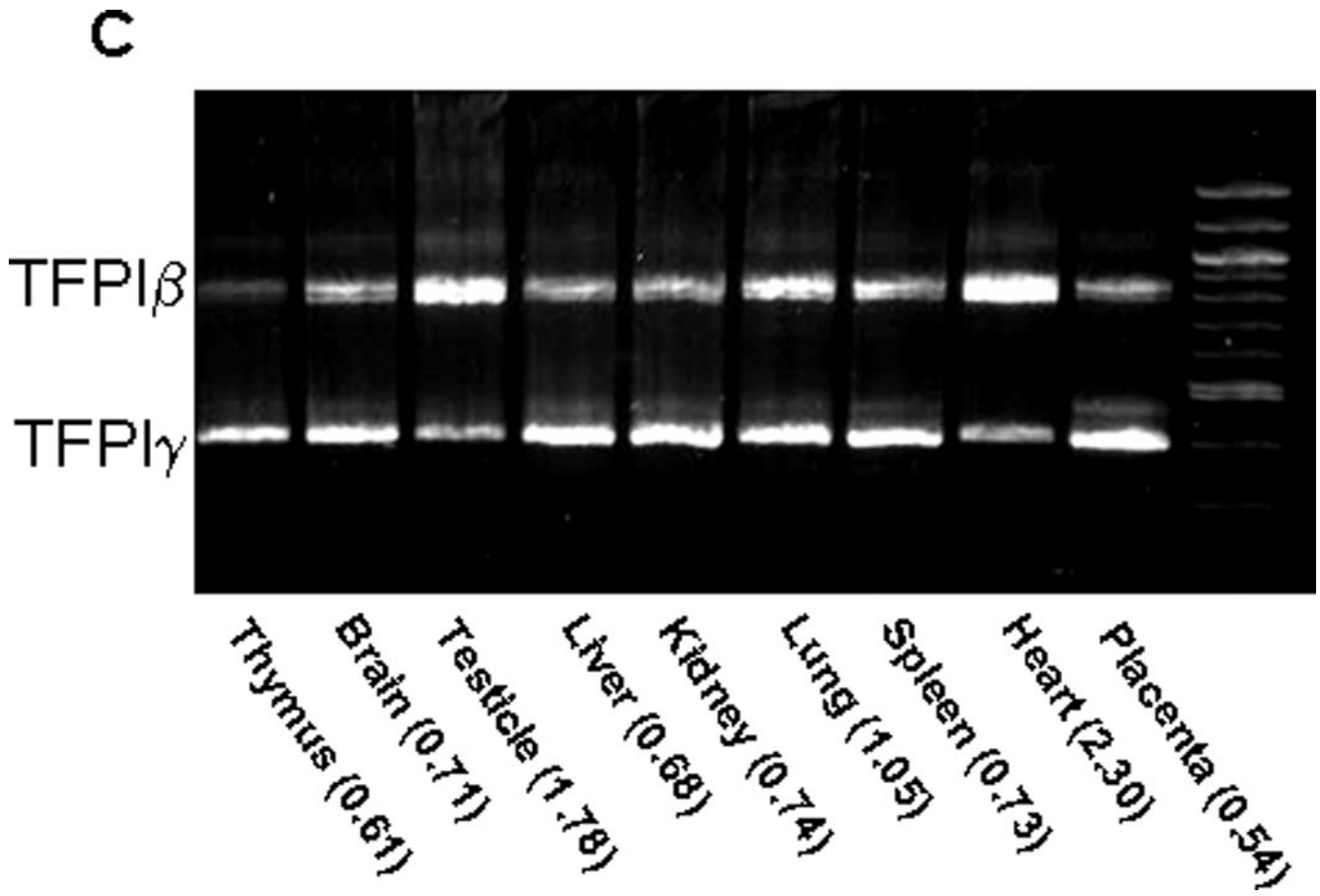

Figure 3.

TFPIα, TFPIβ and TFPIγ mRNA expression in human and mouse tissues. **A)** Quantitative real time PCR analysis of TFPIα and TFPIβ mRNA expression in human and mouse tissues compared to the housekeeper gene RPL-19. The bar graphs represent the average ± SD of 3 to 9 independent experiments performed using human and mouse cDNA. **B)** The ratios of TFPIα to TFPIβ mRNA in human and mouse tissues are presented demonstrating that there is more TFPIα mRNA than TFPIβ mRNA in all human and mouse tissues examined. **C)** cDNA obtained from mouse tissue was used as a template in a PCR reaction with a forward primer in the second Kunitz domain and a reverse primer distal to the TFPIγ region of exon 8. Two products are obtained corresponding to TFPIβ and TFPIγ. The intensity of the bands was quantified by densitometry. The TFPIβ:TFPIγ ratio for each tissue is indicated.

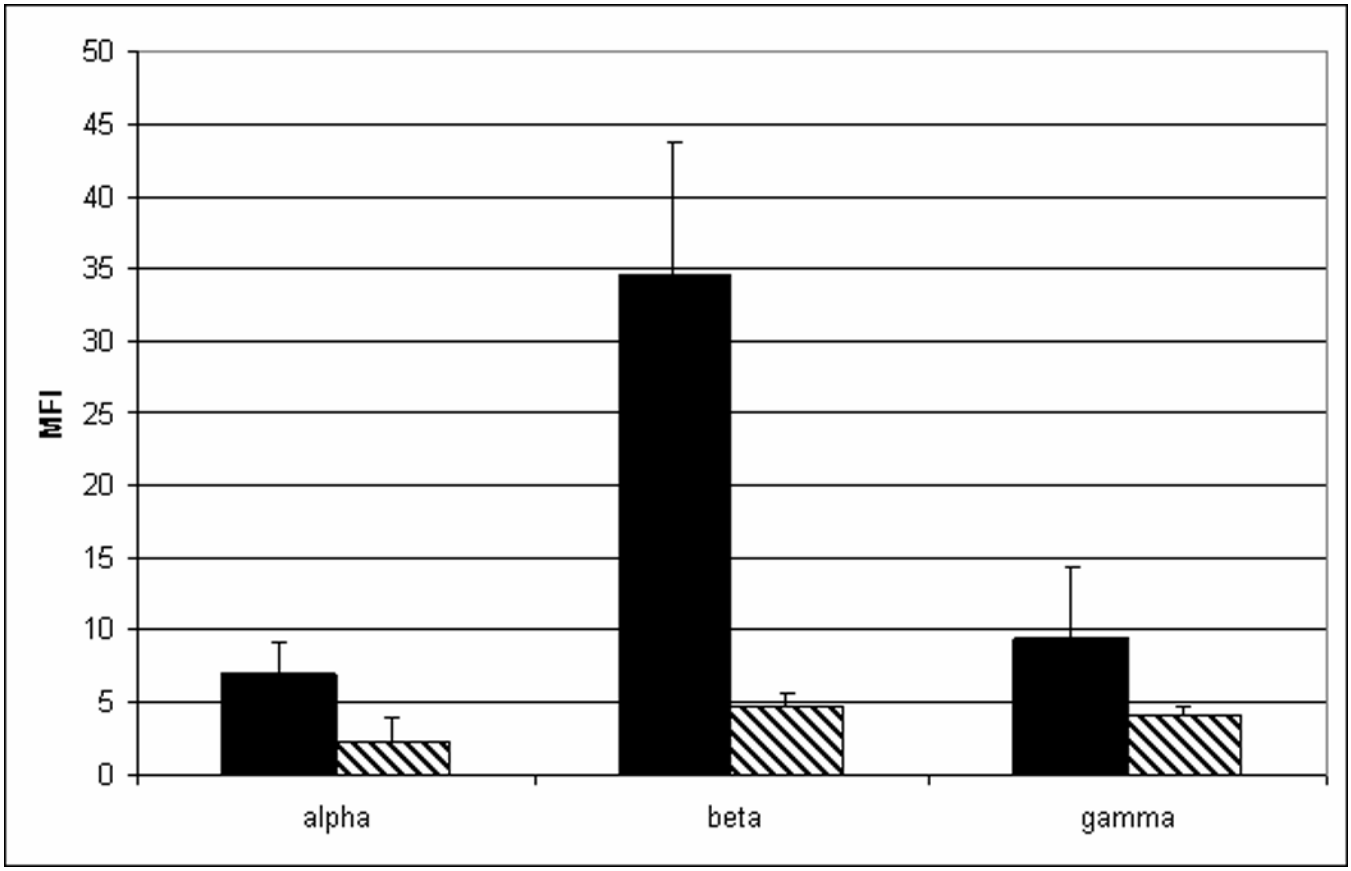

Figure 4.

TFPIγ produced by CHO cells is secreted and inhibits TF-fVIIa activity. **A)** CHO cells were transfected with mouse TFPIα, TFPIβ or TFPIγ and examined for surface TFPI expression using flow cytometry following incubation for 30 min at 37°C in buffer (solid bars) or in the presence of 1 U/ml PIPLC (hatched bars). **B)** The amount of TFPIγ activity in conditioned media (16 h culture) and the PIPLC releasate of CHO cells transfected with TFPIγ was determined in assays that measure in TF-fVIIa activation of fX: (■) Buffer only; (♦) Conditioned media; (▲) PIPLC releasate; (●) Conditioned media in the presence of inhibitory anti-mouse TFPI antibody; (▼) PIPLC releasate in the presence of inhibitory anti-mouse TFPI antibody. **C)** TFPI activity was quantified in conditioned media (16 h culture) and the PIPLC releasate using assays that measure in TF-fVIIa activation of fX. The concentration of TFPI in the media and PIPLC releasate was determined by comparison to a standard curve generated using known amounts of recombinant TFPI and multiplied by the sample volume to obtain the total amount of TFPI in each sample. Data are expressed as the percentage of the TFPI released from the cell surface by PIPLC (average ± SD of three experiments).

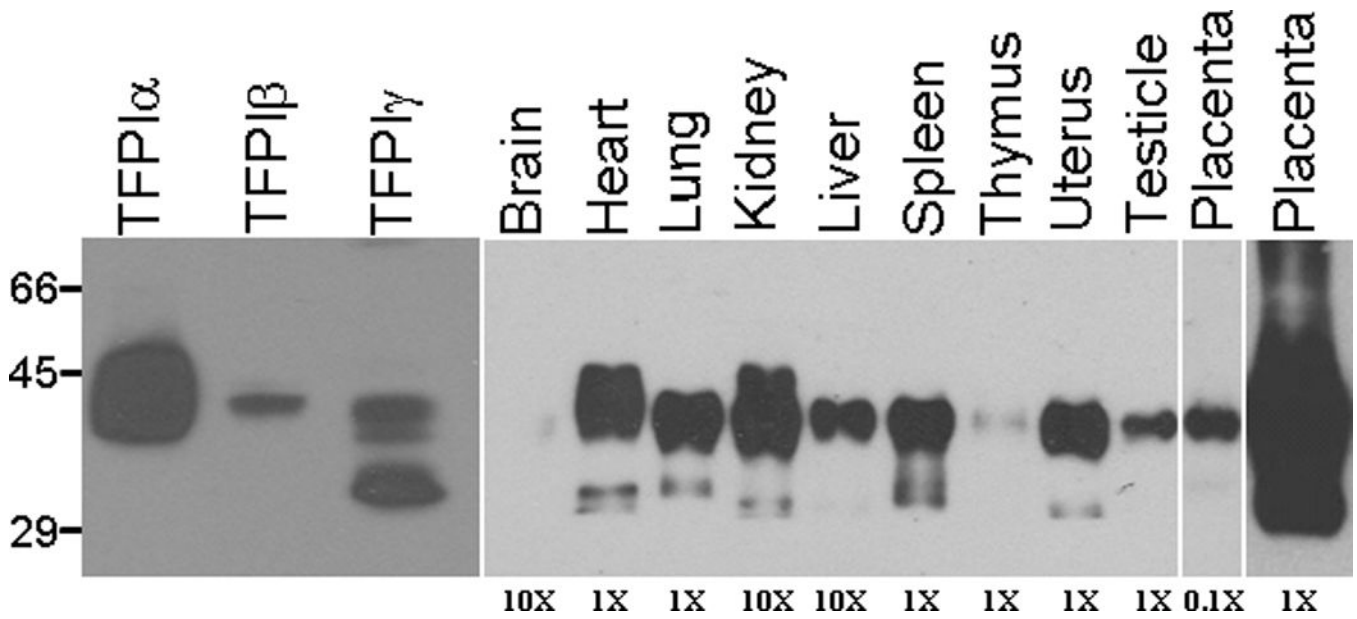

Figure 5.

Western blot analysis of TFPI in mouse tissues. Mouse tissues were lysed in CHAPS buffer, protein standardized and subjected to SDS-PAGE and western blot analysis for TFPI. The relative amount of total protein from each tissue loaded on the gel is indicated at the bottom of the gel. TFPIα, TFPIβ and TFPIγ from transfected CHO cells were also subjected to SDS-PAGE and western blot analysis for comparison with the tissue blots.

Table 1

Primers used for PCR reactions

Human 3' RACE	
Exon 6 outer	5'-TGG GCA ATA TGA ACA ATT TTG AGA CAC-3'
Exon 6 inner	5'-GGA ATA TGT CGA GGT TAT ATT ACC AGG T-3'
Exon 9 outer	5'-GTG GAT GTG GGG GAA ATG AAA-3'
Exon 9 inner	5'-CTT CCA AAC AAG AAT GTC TGA GGG CAT-3'
Mouse 3' RACE	
Exon 6 outer	5'-GAA AGG CCA GAT TTC TGC TTC TTG GAA GAG-3'
Exon 7 inner	5'-CCC AGT CTC CCA AAG TGC CCA GGC GTC GGG-3'
Primers used in Figures 2 and 3C	
Human K2 forward	5'-GGA ATA TGT CGA GGT TAT ATT ACC AGG T-3'
Human K3 reverse	5'-GGC GGC ATT TCC CAA TGA CTG AAT-3'
Human Exon 8 reverse	5'-TGC ATG TAA ATA TTA AAA CTT TAT TAG-3'
Mouse K2 forward	5'-CCT GGG CAA CCG CAA CAA CTT-3'
Mouse K3 reverse	5'-CAT GAT CTC AGA CAT CTC CTT CTG-3'
Mouse Exon 8 reverse	5'-TGG CCA CAG GGT CTT CTT TAT TAC ATC T-3'
Real time PCR	
Human TFPIα forward	5'-ATT TCA CGG TCC CTC ATG GTG TCT-3'
Human TFPIα reverse	5'-GGC GGC ATT TCC CAA TGA CTG AAT-3'
Human TFPIβ forward	5'-GAA GGA ACA AAT GAT GGT TGG AAG AAT GCG-3'
Human TFPIβ reverse	5'-ATG GAT GCA TGA ATG CAG AAG GCG-3'
Mouse TFPIα forward	5'-CAA TTC AGC CAC TGG GAA ATG C-3'
Mouse TFPIα reverse	5'-CAT GAT CTC AGA CAT CTC CTT CTG-3'
Mouse TFPIβ forward	5'-CCC AGT CTC CCA AAG TGC CCA GGC GTC GGG-3'
Mouse TFPIβ reverse	5'-GAC GGA ACT CAG AAA GCC TTG GTA-3'